

NLO Lecture 6: Phase Matching

**4.3 Wave propagation in linear non-isotropic media
(repetition)**

4.4 Phase matching

4.4.1 Birefringent phase matching

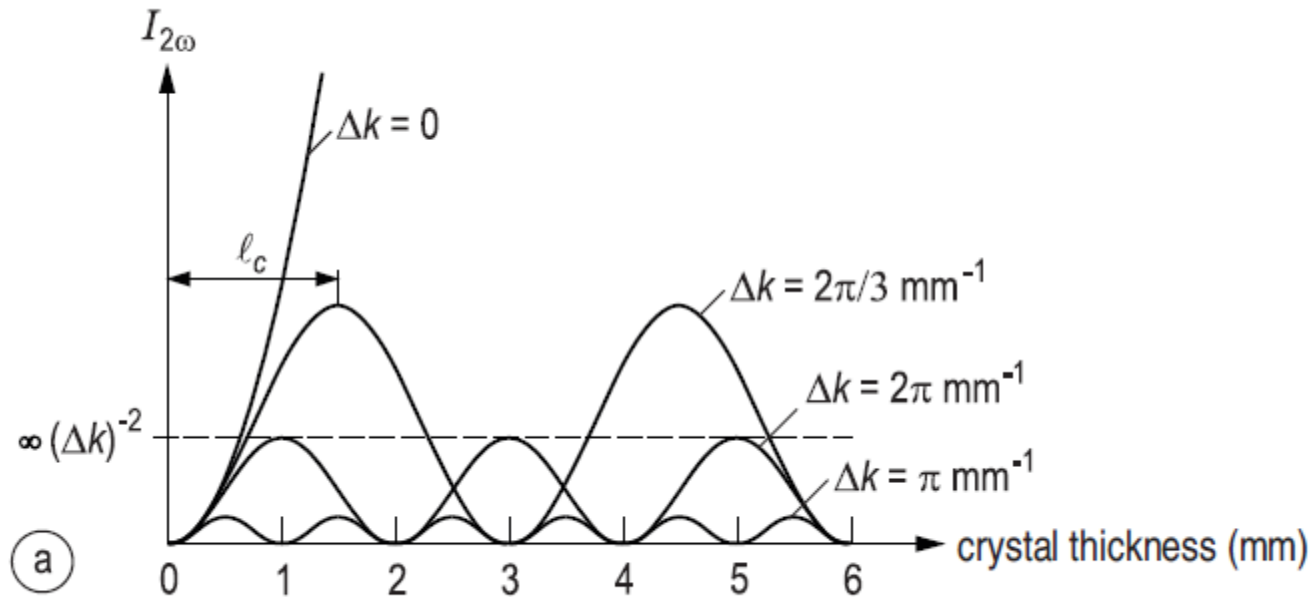
4.4.2 Frequency doubling of Gaussian beams

...

Later:

Quasi-Phasematching in periodically poled crystals, fibers, waveguides, Bragg-structures

Reminder SHG



$$I(2\omega, l) = \frac{2\omega^2 d_{eff}^2}{n_{2\omega} n_{\omega}^2 c_0^3 \epsilon_0} l^2 I^2(\omega) \left[\frac{\sin \Delta k l / 2}{\Delta k l / 2} \right]^2$$

$$l_c = \pi |k(2\omega) - 2k(\omega)|^{-1} = \frac{\lambda(\omega)}{4(n(2\omega) - n(\omega))}.$$

4.3 Wave propagation in linear non-isotropic media

$$\begin{aligned}\mathbf{\ddot{D}} &= \varepsilon \mathbf{\ddot{E}} \\ \varepsilon &= \varepsilon_0 \begin{bmatrix} \varepsilon_x & 0 & 0 \\ 0 & \varepsilon_y & 0 \\ 0 & 0 & \varepsilon_z \end{bmatrix} \\ \nabla \times \nabla \times \hat{\mathbf{E}} &= -\omega^2 \mu_0 \varepsilon \hat{\mathbf{E}}\end{aligned}\tag{4.21}$$

Wave propagation in linear non-isotropic media

As in isotropic media, there are plane-wave solutions with

$$\hat{\mathbf{E}} = \hat{\mathbf{E}}_0 e^{-j\mathbf{k}\cdot\mathbf{r}} \quad (4.22)$$

that obey

$$\mathbf{k} \times \mathbf{k} \times \hat{\mathbf{E}} = -\omega^2 \mu_0 \underset{\text{Tensor}}{\boldsymbol{\epsilon}} \hat{\mathbf{E}} \quad (4.23)$$

The wave vector is orthogonal to the displacement vector but in general not anymore to the electric field

$$\mathbf{k} \perp (\boldsymbol{\epsilon} \hat{\mathbf{E}} = \hat{\mathbf{D}}).$$

From Faraday's law we have

$$j\mathbf{k} \times \hat{\mathbf{E}} = -\omega \hat{\mathbf{B}} \quad (4.24)$$

and therefore, as in the isotropic case, we have

$$\mathbf{k} \perp \hat{\mathbf{B}} \parallel \hat{\mathbf{H}}.$$

$\hat{\mathbf{E}} \parallel \hat{\mathbf{D}}$: only when propagation parallel to a main axis

Poynting vector $\mathbf{S} = \mathbf{E} \times \mathbf{H}$, is always normal to \mathbf{E} and \mathbf{H}
not necessarily parallel to the wave vector

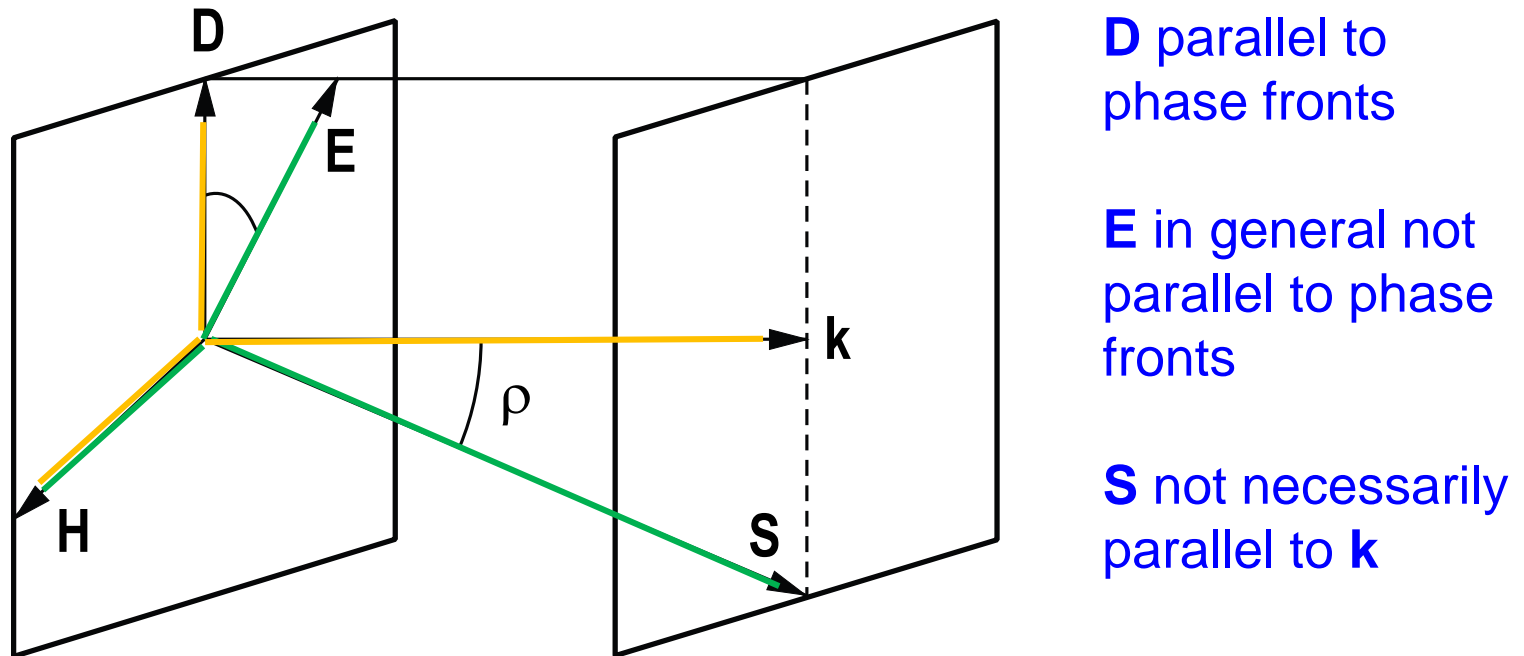


Figure 4.3: Relationship between field vectors, wave vector and Poynting vector of a plane wave in birefringent media.

Form of dielectric susceptibility tensor

isotropic	$\begin{bmatrix} xx & 0 & 0 \\ 0 & xx & 0 \\ 0 & 0 & xx \end{bmatrix}$	cubic
uniaxial e.g. Beta Barium Borate (BBO) Lithium Niobate (LN)	$\begin{bmatrix} xx & 0 & 0 \\ 0 & xx & 0 \\ 0 & 0 & zz \end{bmatrix}$	tetragonal
		trigonal
		hexagonal
biaxial	$\begin{bmatrix} xx & 0 & 0 \\ 0 & yy & 0 \\ 0 & 0 & zz \end{bmatrix}$	orthorhombic
	$\begin{bmatrix} xx & 0 & xz \\ 0 & yy & 0 \\ xz & 0 & zz \end{bmatrix}$	monoclinic
	$\begin{bmatrix} xx & xy & xz \\ xy & yy & yz \\ xz & yz & zz \end{bmatrix}$	triclinic

Table 4.1: Form of the dielectric susceptibility tensor for the different crystal systems.

In the following, we consider the uniaxial case

$$\varepsilon_{xx} = \varepsilon_{yy} = \varepsilon_1 \neq \varepsilon_{zz} = \varepsilon_3$$

The corresponding refractive indices are called ordinary and extraordinary indices.

$$n_1 = n_o \neq n_3 = n_e.$$

Further one distinguishes between positive uniaxial, $n_e > n_o$, and negative uniaxial, $n_e < n_o$, crystals.

Propagation different from main axes

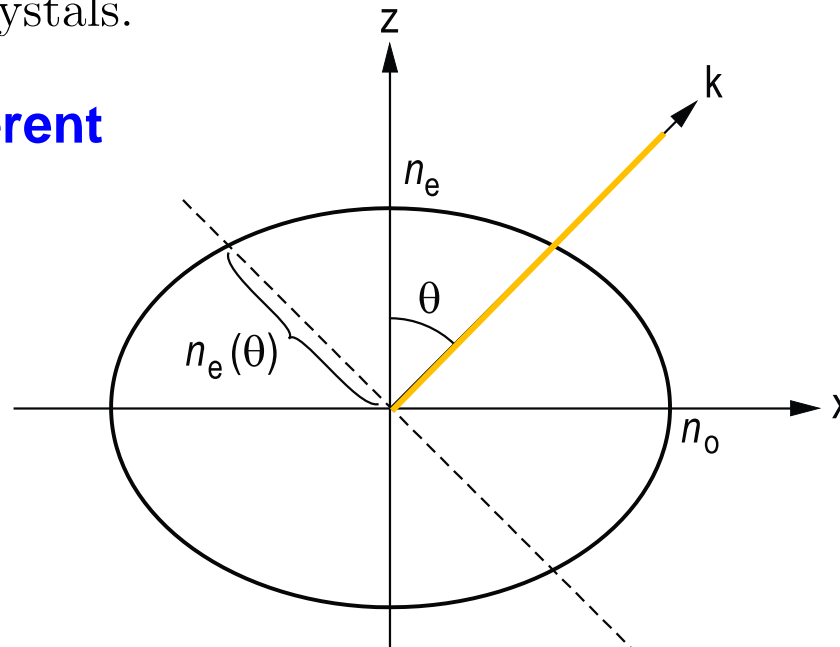


Figure 4.4: Index ellipsoid

Nonlinear optical susceptibilities

generality, we assume the wave vector lies in the x-z-plane. If we inspect Eq. (4.23) closer, we find with $\mathbf{A} \times (\mathbf{B} \times \mathbf{C}) = (\mathbf{A} \cdot \mathbf{C}) \mathbf{B} - (\mathbf{A} \cdot \mathbf{B}) \mathbf{C}$

$$\mathbf{k} \times \mathbf{k} \times \hat{\mathbf{E}} = -\omega^2 \mu_0 \varepsilon \hat{\mathbf{E}}$$

$$\left(\mathbf{k} \cdot \hat{\mathbf{E}} \right) \mathbf{k} - k^2 \hat{\mathbf{E}} + \omega^2 \mu_0 \varepsilon \hat{\mathbf{E}} = \mathbf{0}. \quad \text{(Possible polarizations)} \quad (4.25)$$

$$\begin{pmatrix} k_0^2 n_o^2 + k_x^2 - k^2 & k_x k_z \\ k_z k_x & k_0^2 n_o^2 - k^2 \end{pmatrix} \hat{\mathbf{E}} = \mathbf{0} \quad (4.26)$$

y-polarized wave decouples → ordinary wave $k^2 = k_0^2 n_o^2$.

As the wave in an isotropic medium, it is purely transversal, $\mathbf{k} \perp \hat{\mathbf{E}} \perp \hat{\mathbf{H}}$.

Wave in the x-z plane with polarization in x-z plane: extraordinary wave

$$\det \begin{vmatrix} k_0^2 n_o^2 + k_x^2 - k^2 & k_x k_z \\ k_z k_x & k_0^2 n_e^2 + k_z^2 - k^2 \end{vmatrix} = 0$$

or after some brief transformations

$$\frac{k_z^2}{n_o^2} + \frac{k_x^2}{n_e^2} = k_0^2. \quad (4.27)$$

With $k_x = k \sin(\theta)$, $k_z = k \cos(\theta)$ and $k = n(\theta) k_0$ we obtain for the refractive index of the extraordinary wave

$$\frac{1}{n(\theta)^2} = \frac{\cos^2(\theta)}{n_o^2} + \frac{\sin^2(\theta)}{n_e^2}. \quad (4.28)$$

$$\mathbf{v}_g = \nabla_{\mathbf{k}} \omega(\mathbf{k}) \parallel \mathbf{S},$$

**normal to index ellipsoid and
parallel to Poynting vector**

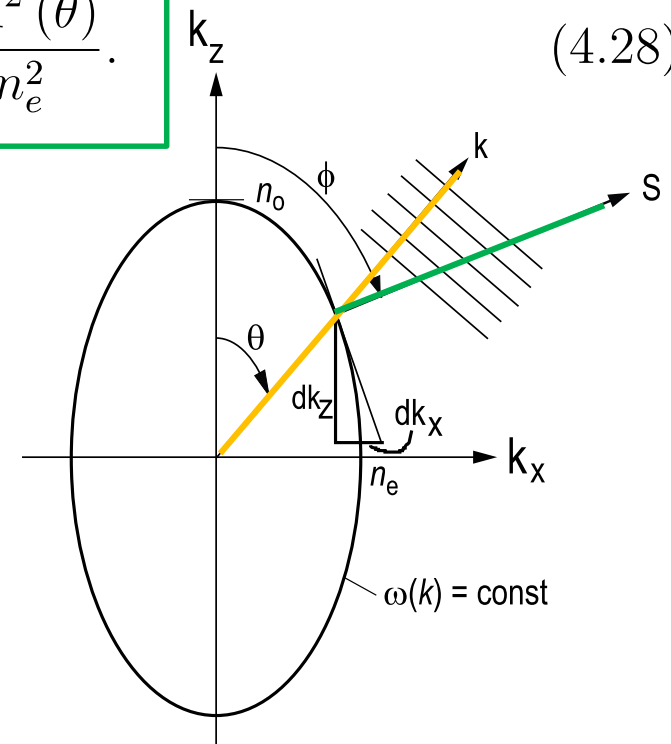


Figure 4.5: Cut through the surface of the index ellipsoid with constant free-space value $k_0(k_x, k_y, k_z)$ or frequencies.

and is normal to the index ellipsoid. To determine the “walk-off” angle between the Poynting vector and the wave vector, we consider

$$\tan \theta = \frac{k_x}{k_z}$$

$$\tan \phi = -\frac{dk_z}{dk_x}.$$

From $\frac{k_z^2}{n_o^2} + \frac{k_x^2}{n_e^2} = k_0^2$ we find

$$\frac{2k_z dk_z}{n_o^2} + \frac{2k_x dk_x}{n_e^2} = 0, \quad (4.29)$$

and

$$\tan \phi = \frac{n_o^2 k_x}{n_e^2 k_z} = \frac{n_o^2}{n_e^2} \tan \theta.$$

Therefore, we obtain for the walk-off angle between Poynting vector and wave number vector

$$\tan \varrho = \tan (\theta - \phi) = \frac{\tan \theta - \tan \phi}{1 + \tan \theta \tan \phi} \quad (4.30)$$

$$\tan \varrho = \frac{\left(1 - \frac{n_o^2}{n_e^2}\right) \tan \theta}{1 + \frac{n_o^2}{n_e^2} \tan^2 \theta}.$$

Intermediate Summary

- \mathbf{k} not same direction as \mathbf{S} (“walk-off”)
- Refractive index depends on polarization and angle θ between \mathbf{k} and optical axis (\mathbf{z}):
 $n_o, n_e(\theta)$

4.4 Phase matching

4.4.1 Birefringent phase matching

In SHG, we introduced the coherence length

$$\ell_c = \pi |k(2\omega) - 2k(\omega)|^{-1} = \frac{\lambda(\omega)}{4(n(2\omega) - n(\omega))}.$$

coherence length may be as short as a few microns, if fundamental and second harmonic have the same polarization.

Propagation along main axis with orthogonal polarization (and zero-walkoff angles)

non-critical phase matching

here: for neg. birefringence, similar for pos. birefringence

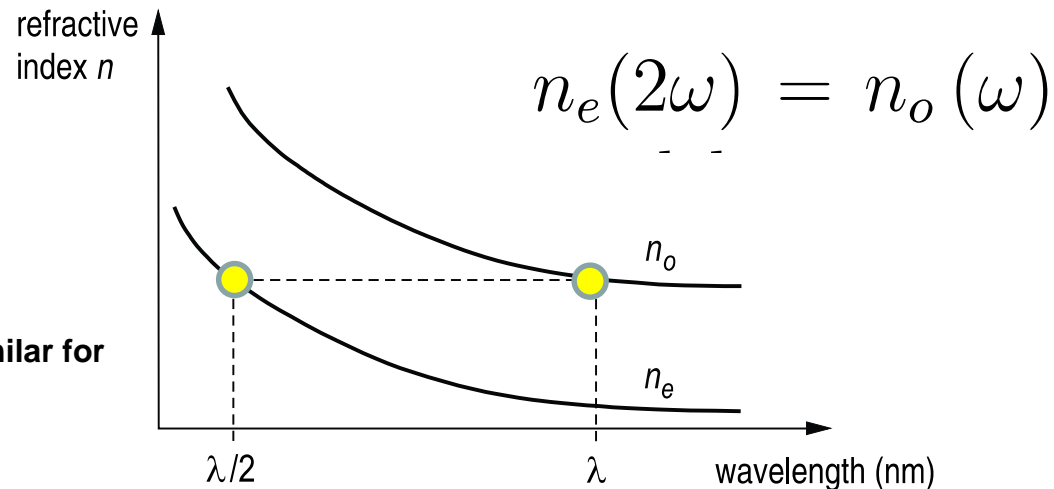


Figure 4.6: Non-critical phase matching

only approximately. Often this can be further matched by temperature tuning. Important examples for this technique is the frequency doubling of $1.06\text{-}\mu\text{m}$ radiation in LiNbO_3 , CD^*A and LBO or frequency doubling of 530-nm light in KDP.

Type-I critical phase matching

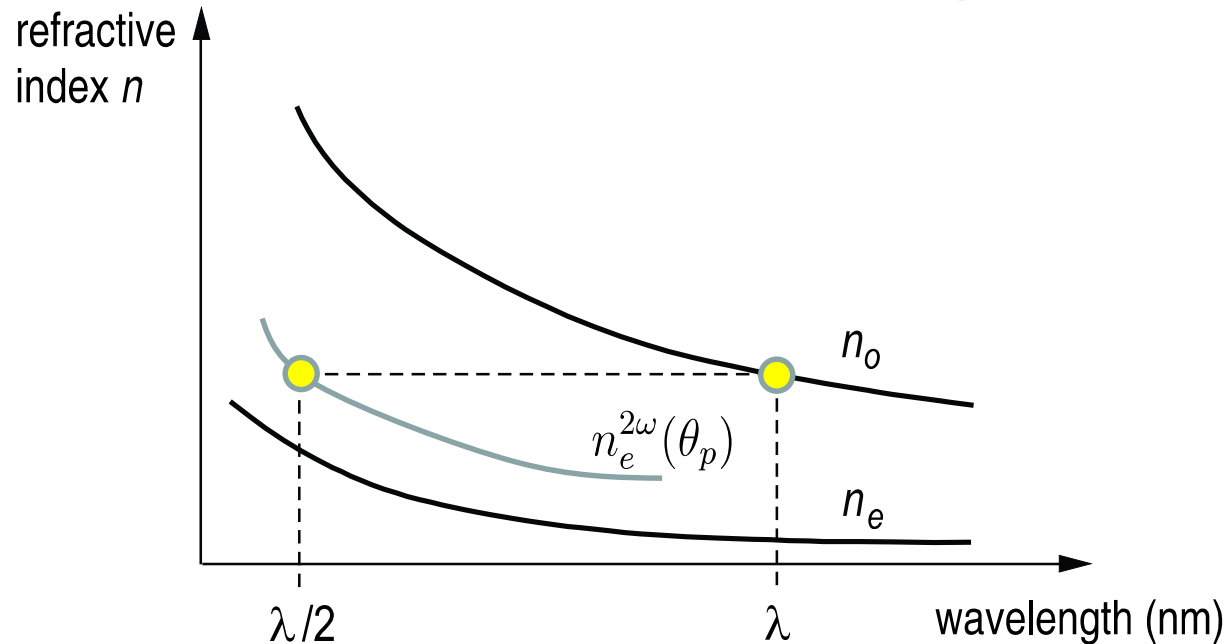


Figure 4.7: Type-I critical phase matching.

A more general situation is shown in Fig. 4.7. The birefringence is too strong for non-critical phase matching. However, by angle-tuning with respect to the optical axis every index value between $n_e(2\omega)$ and $n_o(2\omega)$ can be dialed in, especially $n_o(\omega)$. This phase matching angle, θ_p , is determined by

$$n_e^{2\omega}(\theta_p) = \left\{ \frac{\sin^2 \theta_p}{(n_e^{2\omega})^2} + \frac{\cos^2 \theta_p}{(n_o^{2\omega})^2} \right\}^{-1/2} = n_o^\omega \quad \begin{array}{l} \text{for } \theta_p = 90\text{deg} \\ \text{---> Non-critical phase} \\ \text{matching} \end{array}$$

which leads to

$$\tan \theta_p = \frac{n_e^{2\omega}}{n_o^{2\omega}} \sqrt{\frac{(n_o^\omega)^2 - (n_o^{2\omega})^2}{(n_e^{2\omega})^2 - (n_o^\omega)^2}}$$

Walk-off angle (between fundamental and harmonic propagation direction)

$$\tan \rho = \frac{(n_o^\omega)^2}{2} \left\{ \frac{1}{(n_e^{2\omega})^2} - \frac{1}{(n_o^{2\omega})^2} \right\} \sin 2\theta_p \approx \frac{\Delta n}{n} \sin 2\theta_p$$

only valid for small birefringence

Walk - Off

$$\tan \rho = \frac{(n_0^\omega)^2}{2} \left\{ \frac{1}{(n_e^{2\omega})^2} - \frac{1}{(n_0^{2\omega})^2} \right\} \sin 2\theta_p \approx \frac{\Delta n}{n} \sin 2\theta_p$$

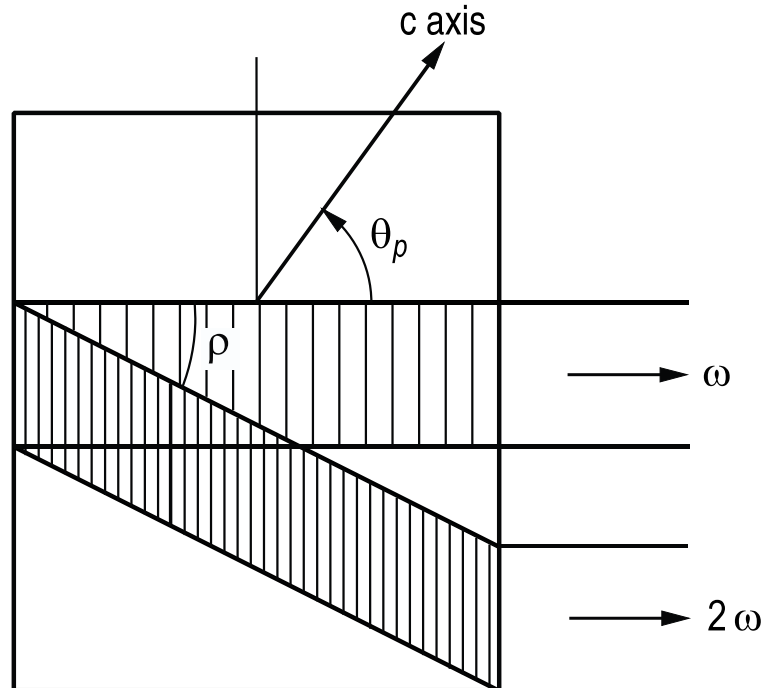
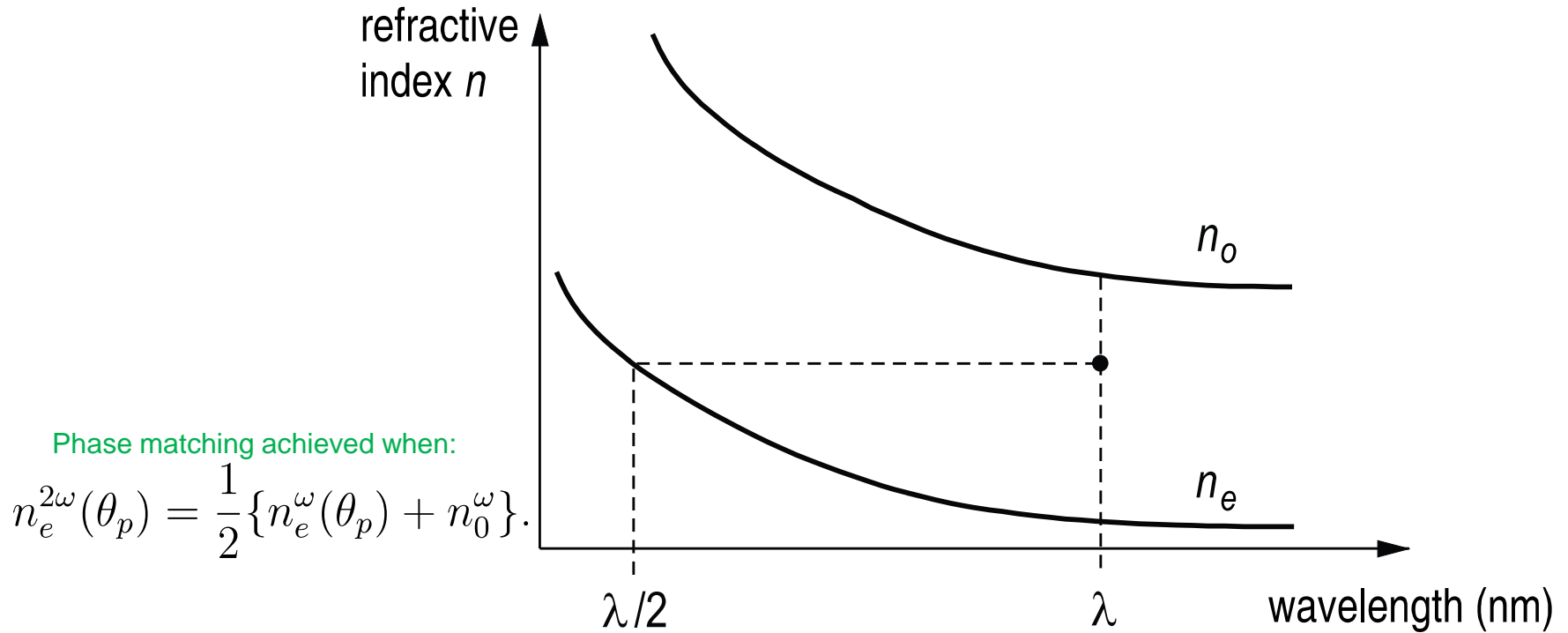


Figure 4.8: Walk-off between ordinary and extraordinary wave.

Gaussian beam with $w_0 \rightarrow$ walk-off length

$$\ell_a = \frac{\sqrt{\pi}}{\rho} w_0.$$

Type-II phase matching



	Type I	Type II
$n_e < n_o$ (neg. uniaxial) :	$oo \rightarrow e$	$oe \rightarrow e$
$n_e > n_o$ (pos. uniaxial) :	$ee \rightarrow o$	$oe \rightarrow o$

Table 4.2: Phase-matching configurations

Acceptance angle

$$\begin{aligned}\Delta k &= \cancel{(k_{2\omega} - 2k_\omega)}|_{\theta_p} + \frac{d}{d\theta} (k_{2\omega} - 2k_\omega) \Big|_{\theta_p} \Delta\theta + \dots \\ &= \frac{4\pi\Delta\theta}{\lambda} \left\{ \frac{dn_{2\omega}(\theta)}{d\theta} - \frac{dn_\omega}{d\theta} \right\}_{\theta_p}\end{aligned}$$

For type-I phase matching, there is $dn_\omega/d\theta = dn_o^\omega/d\theta = 0$ and

$$n_{2\omega}(\theta) = \left\{ \frac{\sin^2 \theta}{(n_e^{2\omega})^2} + \frac{\cos^2 \theta}{(n_o^{2\omega})^2} \right\}^{-1/2}.$$

The angle-induced phase mismatch can then be rewritten as

$$\begin{aligned}\Delta k &= -\frac{2\pi\Delta\theta}{\lambda} n_{2\omega}(\theta)^3 \left\{ \frac{2 \sin \theta \cos \theta}{(n_e^{2\omega})^2} - \frac{2 \sin \theta \cos \theta}{(n_o^{2\omega})^2} \right\} \\ &= \frac{2\pi\Delta\theta}{\lambda} (n_o^\omega)^3 \left\{ \frac{1}{(n_o^{2\omega})^2} - \frac{1}{(n_e^{2\omega})^2} \right\} \sin 2\theta_p.\end{aligned}$$

For a given crystal length ℓ the phase mismatch should not be larger than the half-width at half-maximum (HWHM) of the sinc^2 -function, i.e., $\Delta k = \pi/\ell$,

For a given crystal length ℓ the phase mismatch should not be larger than the half-width at half-maximum (HWHM) of the sinc^2 -function, i.e., $\Delta k = \pi/\ell$,

$$\Delta\theta = \frac{\lambda}{2\ell \sin 2\theta_p} (n_o^\omega)^{-3} \left\{ \frac{1}{(n_o^{2\omega})^2} - \frac{1}{(n_e^{2\omega})^2} \right\}^{-1}$$

With $\Delta n^{2\omega} = n_o^{2\omega} - n_e^{2\omega}$, $(n_o^{2\omega})^{-2} = (n_e^{2\omega})^{-2} - 2(n_e^{2\omega})^{-3} \Delta n^{2\omega}$ and $n_e^{2\omega} = n_o^\omega$, we obtain

$$\Delta\theta = -\frac{\lambda}{4\ell \sin 2\theta_p \Delta n^{2\omega}}.$$

For most cases $|\Delta\theta|$ is on the order of a few milliradians, e.g., for KH_2PO_4 (KDP) at $\lambda = 1.064 \mu\text{m}$, $n_e^\omega = 1.466$, $n_o^\omega = 1.506$, $n_e^{2\omega} = 1.487$, $n_o^{2\omega} = 1.534$. For this case, the phase-matching angle is $\theta_p = 49.9^\circ$ and for a 1-cm long crystal, there is $|\Delta\theta| = 0.001$.

For type-II phase matching under the condition $n_e^{2\omega}(\theta_p) = [n_e^\omega + n_o^\omega]/2$, we obtain

$$\Delta k = \frac{2\pi\Delta\theta}{\lambda} \left\{ 2 \frac{dn_e^{2\omega}(\theta)}{d\theta} - \frac{dn_e^\omega(\theta)}{d\theta} \right\}_{\theta_p} \quad (4.32)$$

Weak birefringence

For weak birefringence and if the wavelength dependence of both indices is similar, than the acceptance angle is roughly twice as large as for type-I phase matching. For non-critical phase matching, that is 90°-phase matching, the above derivation can not be used, since the phase-matching error depends second order on the acceptance angle. One finds

$$\Delta k = \frac{2\pi}{\lambda} (n_o^\omega)^3 \left\{ \frac{1}{(n_e^{2\omega})^2} - \frac{1}{(n_o^{2\omega})^2} \right\} (\Delta\theta)^2 \quad (4.33)$$

which simplifies for small birefringence to

$$\Delta\theta \approx \left\{ \frac{\lambda}{2\ell\Delta n^{2\omega}} \right\}^{1/2} \quad (4.34)$$

For $\lambda = 1 \mu\text{m}$, $\Delta n = 0.047$ and $\ell = 1 \text{ cm}$, we find $|\Delta\theta| = 0.02$, e.g., this acceptance angle is an order of magnitude higher than for critical phase matching, which justifies the names critical and non-critical phase matching.

Acceptance bandwidth

$$\Delta k = \{k_{2\omega} - 2k_{\omega}\}|_{\lambda_p} + \left\{ \frac{d}{d\lambda} (k_{2\omega} - 2k_{\omega}) \right\}_{\lambda_p} \Delta\lambda + \dots \quad (4.35)$$

$$\approx 4\pi\Delta\lambda \left\{ \frac{d}{d\lambda} \left(\frac{n_{2\omega}}{\lambda} - \frac{n_{\omega}}{\lambda} \right) \right\}_{\lambda_p} = 4\pi \frac{\Delta\lambda}{\lambda} \left\{ \frac{1}{2} \frac{dn_{2\omega}}{d(\lambda/2)} - \frac{dn_{\omega}}{d\lambda} \right\}_{\lambda_p} \quad (4.36)$$

$$= 4\pi \frac{\Delta\lambda}{\lambda} \left\{ \frac{1}{2} \frac{dn}{d\lambda} \Big|_{2\omega} - \frac{dn}{d\lambda} \Big|_{\omega} \right\} \quad (4.37)$$

The acceptance bandwidth follows again from the condition, that the phase mismatch over the propagation length must stay smaller than the HWHM of the sinc²- function, i.e., $|\Delta k| < \pi/\ell$ or

$$\Delta\lambda = \left| \frac{\lambda}{4\ell} \left\{ \frac{1}{2} \frac{dn}{d\lambda} \Big|_{2\omega} - \frac{dn}{d\lambda} \Big|_{\omega} \right\}^{-1} \right|, \quad (4.38)$$

where λ is the wavelength of the fundamental wave and ℓ the interaction length. The other way around, if a bandwidth $2\Delta\lambda$ needs to be frequency doubled, a phase matched crystal can only have the length ℓ

$$\ell = \frac{\lambda}{2\Delta\lambda} \left\{ \frac{1}{2} \frac{dn}{d\lambda} \Big|_{2\omega} - \frac{dn}{d\lambda} \Big|_{\omega} \right\}^{-1} \quad (4.39)$$

Acceptance bandwidth... when frequency doubling a pulse (temporal overlap)

its second harmonic. The group velocity of a pulse is given by

$$v_g = \frac{d\omega}{dk} = \frac{d}{dk} \left(\frac{c}{n} k \right) = \frac{c}{n} - \frac{ck}{n^2} \frac{dn}{d\lambda} \frac{d\lambda}{dk} \quad (4.40)$$

where

$$\begin{aligned} \frac{d\lambda}{dk} &= \frac{d}{dk} \left(\frac{2\pi n}{k} \right) = - \left(\frac{2\pi n}{k^2} \right) + \frac{2\pi}{k} \frac{dn}{d\lambda} \frac{d\lambda}{dk} \\ \frac{d\lambda}{dk} &= \frac{- (2\pi n/k^2)}{1 - \frac{2\pi}{k} \frac{dn}{d\lambda}}, \end{aligned} \quad (4.41)$$

that is

$$v_g = \frac{c}{n} \left\{ 1 - \frac{\lambda}{n} \frac{dn}{d\lambda} \right\}^{-1}. \quad (4.42)$$

Two pulses with duration t_p but with different group velocities will overlap over a length

$$\ell \approx \frac{t_p}{2} \left\{ \frac{1}{v_g} \Big|_{\omega} - \frac{1}{v_g} \Big|_{2\omega} \right\}^{-1}.$$

Acceptance bandwidth... when frequency doubling a pulse

With Eq. (4.42) we obtain

$$\Rightarrow \ell \approx \frac{t_p c}{2\lambda} \left\{ \frac{1}{2} \frac{dn}{d\lambda} \Big|_{2\omega} - \frac{dn}{d\lambda} \Big|_{\omega} \right\}^{-1}.$$

Using the time-bandwidth relationship

$$t_p \approx \frac{1}{\Delta f} = \frac{\lambda^2}{c\Delta\lambda} \quad (4.43)$$

we find the maximum crystal length similar to the one derived from the phase matching condition (4.39)

$$\Rightarrow \ell \approx \frac{\lambda}{2\Delta\lambda} \left\{ \frac{1}{2} \frac{dn}{d\lambda} \Big|_{2\omega} - \frac{dn}{d\lambda} \Big|_{\omega} \right\}^{-1}.$$

4.4.2 Frequency doubling of Gaussian beams

A laser emits radiation in a TEM₀₀ - mode, i.e., a Gaussian beam. The electric field of a Gaussian beam is described by

$$\hat{E}(x, y, z) = \hat{E}_0 \frac{w_0}{w(z)} \exp\{-j(kz - \phi)\} \times \exp\left\{-(x^2 + y^2) \left[\frac{1}{w^2(z)} + \frac{jk}{2R(z)} \right]\right\} \quad (4.44)$$

$$w(z) = w_0 \left\{ 1 + \left(\frac{\lambda z}{\pi w_0^2} \right)^2 \right\}^{1/2} \quad (4.45)$$

$$\phi = \underset{(\text{arctan})}{\tan^{-1}} \left\{ \frac{\lambda z}{\pi w_0^2} \right\} \quad (4.46)$$

$$R(z) = z \left\{ 1 + \left(\frac{\pi w_0^2}{\lambda z} \right)^2 \right\} \quad (4.47)$$

Gaussian beam

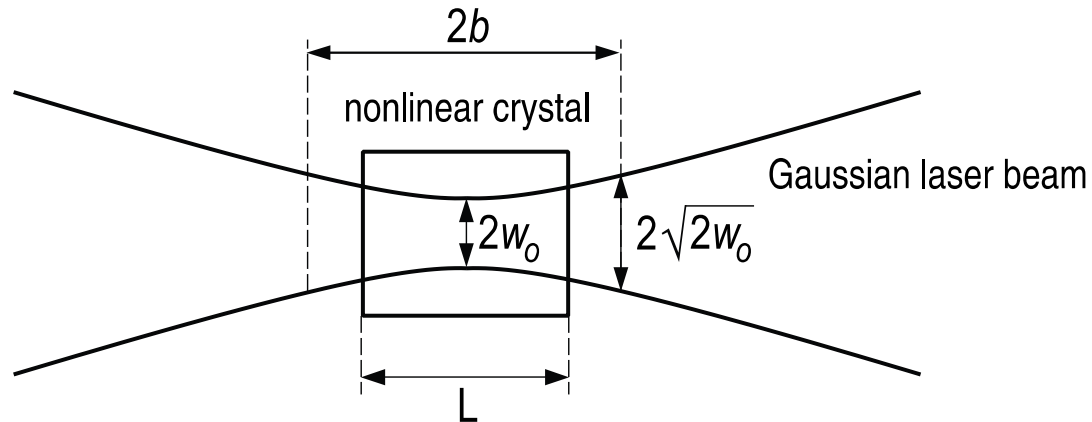


Figure 4.10: Intensity distribution of a Gaussian beam.

The confocal parameter of the beam is twice the Rayleigh range and given by

$$b = \frac{2\pi w_0^2}{\lambda} \quad (4.48)$$

see Fig. 4.10. The Rayleigh range is the distance, over which the beam cross sectional area doubles, $\pi w^2(z) < 2\pi w_0^2$. The opening angle of the beam due to diffraction is

$$\Delta\theta \approx \frac{w(z)}{z} \approx \frac{\lambda}{\pi w_0}. \quad (4.49)$$

Gaussian beam continued

In the near field ($z \ll b$), the beam is close to a plane wave

$$\hat{E}(x, y) = \hat{E}_0 \exp\left(-\frac{x^2 + y^2}{w_0^2}\right) \exp(-jkz) \quad (4.50)$$

or

$$\hat{E}(r) = \hat{E}_0 \exp\left(-\frac{r^2}{w_0^2}\right) \exp(-jkz) \quad (4.51)$$

$$P = \frac{n c \epsilon_0}{2} \int_0^\infty \int_0^{2\pi} |\hat{E}_0|^2 \exp\left(-\frac{2r^2}{w_0^2}\right) r dr d\phi \quad (4.52)$$

$$= \frac{n c \epsilon_0}{2} |\hat{E}_0|^2 \left(\frac{\pi w_0^2}{2}\right) \Rightarrow P = I_0 \left(\frac{\pi w_0^2}{2}\right), \quad (4.53)$$

with the peak intensity $I_0 = \frac{n c \epsilon_0}{2} |\hat{E}_0|^2$ on beam axis. The effective area, A_{eff} , of a Gaussian beam is therefore

$$A_{eff} = \frac{P}{I_0} = \frac{\pi w_0^2}{2}. \quad (4.54)$$

Gaussian beam continued

Plane wave with radial beam profile: $\hat{E}(r) = \hat{E}_0 \exp\left(-\frac{r^2}{w_0^2}\right) \exp(-jkz)$

$$\hat{E}_2(r, \ell) = -\frac{j\omega_1 d_{eff}}{n_{2\omega} c} \hat{E}_1^2(r) \ell = -j\kappa \hat{E}_1^2(r) \ell$$

where we introduced the interaction coefficient $\kappa = \frac{\omega_1 d_{eff}}{n_{2\omega} c} = \frac{\omega_2 d_{eff}}{2n_{2\omega} c}$.
Gaussian shape for the second harmonic

$$\hat{E}_2(r, \ell) = -j\kappa \hat{E}_1^2 \ell e^{-2r^2/w_1^2}.$$

The frequency-doubled beam shows only half the cross section compared to the fundamental beam $w_2 = w_1/\sqrt{2}$ or the confocal parameter $b_2 = \pi w_2^2/(\lambda/2) = \pi w_1^2/\lambda = b_1$. Thus the confocal parameters of both beams are the same. The total generated power at 2ω is

$$P_2 = \frac{n_{2\omega} c \varepsilon_0}{2} \int_0^{2\pi} \int_0^\infty |\hat{E}_2(r)|^2 r dr d\phi = \frac{n_{2\omega} c \varepsilon_0}{2} \kappa^2 \hat{E}_1^4 \ell^2 \left(\frac{\pi w_1^2}{4}\right) \quad (4.57)$$

$$= \frac{n_{2\omega}}{n_\omega} P_1 \kappa^2 \hat{E}_1^2 \ell^2 / 2 \quad (4.58)$$

Estimate of conversion efficiency for Gaussian beam

similar to the case of plane waves. From Eq. (4.59) we obtain for the conversion efficiency

$$\eta = \frac{P_2}{P_1} = \frac{2\omega^2}{\varepsilon_0 c^3} \left(\frac{d_{eff}^2}{n^3} \right) \left(\frac{P_1}{\pi w_1^2} \right) \cdot \ell^2. \quad (4.61)$$

Thus the conversion efficiency is proportional to (d_{eff}^2/n^3) . Thus for choosing a crystal for efficient frequency doubling, not only the effective nonlinearity d_{eff} should be as high as possible, but simultaneously, the refractive index n should be small. Fig. 4.11 gives an overview over the figure of merit defined by $FOM = d_{eff}^2/n^3$. From Fig. 4.10 we see that for $\ell > b$ the beam cross section increases and the conversion drops. A numerical optimization without any approximations results in the crystal length $\ell = 2.84 \cdot b$ for maximum conversion. With this result and $b = 2\pi w_1^2/\lambda$, we obtain for the maximum conversion efficiency

$$\eta_{opt} = \frac{P_2}{P_1} = \frac{2\omega^2}{\varepsilon_0 \lambda c^3} \left(\frac{d_{eff}^2}{n^3} \right) 5.68 P_1 \cdot \ell. \quad (4.62)$$

The weaker the focus and the longer the crystal, the larger is the conversion in a $\chi^{(2)}$ -process, if phase matching is maintained over the full length.

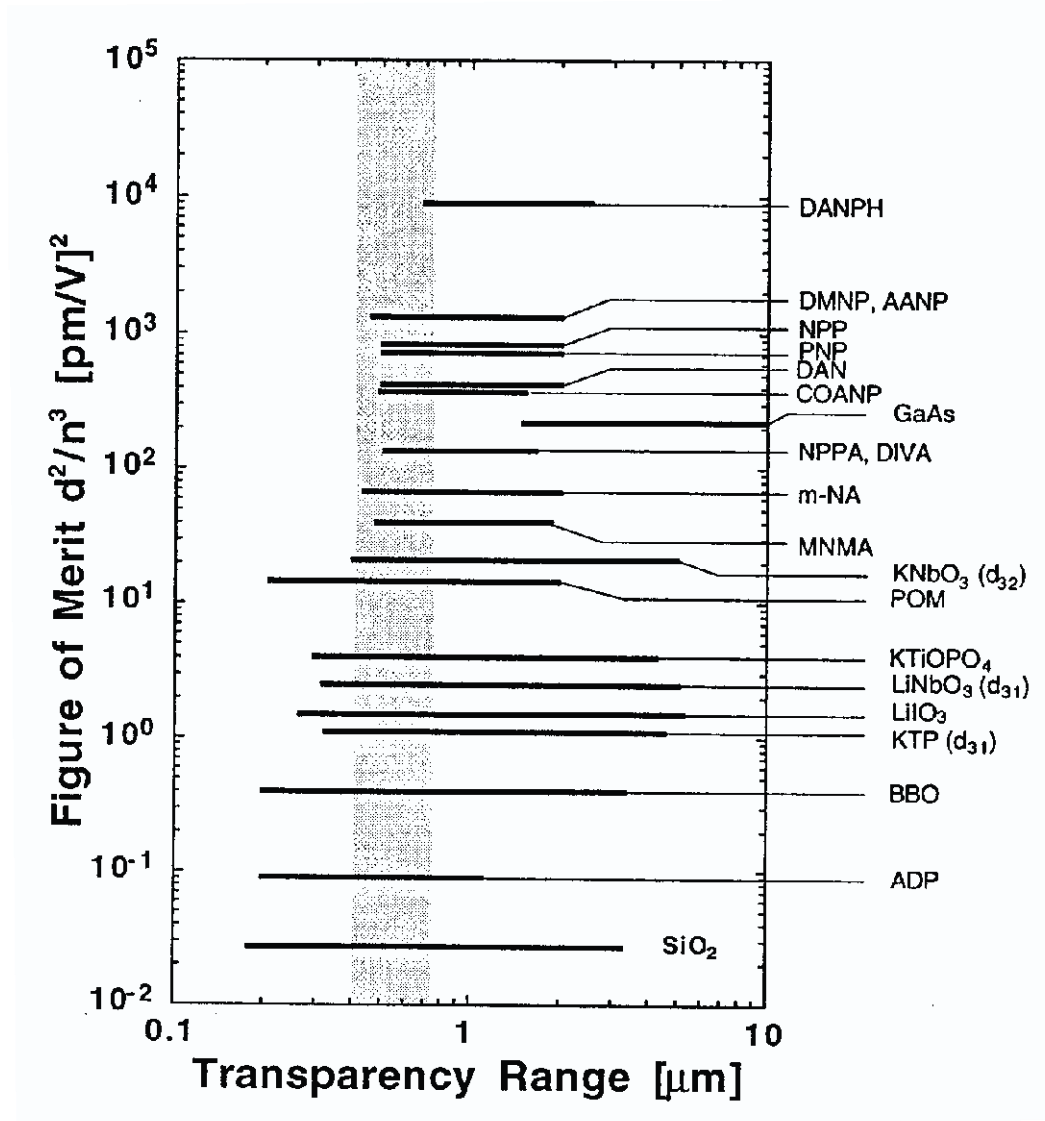


Figure 4.11: Figure of merit (FOM) for different nonlinear optical materials.